

Chapter 48

Designing of DC Microgrid with Fast Charging Converter and Control for Solar PV, Fuel Cell and Battery-Integrated Charging Station



Dheeraj Kumar Dhaked, Mayank Singh, and Dinesh Birla

Abstract Sustainable and environment-friendly transportation is need of the hour, and electrical vehicles (EV) are the only option for that. Slow charging time, lesser charging stations and grid instability are major cause for slow growth rate of EV. This charging station aims to reduce the dependency on grid during peak load time, and it will also be helpful where the grid power is not available. This paper has employed a high gain, fast charging DC/DC converter with controller for charging station of EV which contains solar PV, fuel cells (FC) and battery energy storage system (BESS). The converter and its controllers performance are validated with different renewable sources using MATLAB/Simulink tool, and the results for battery charging are presented along with dynamic response. The observed results are satisfactory for validation which gives higher charging current that led to less charging time.

Keywords Microgrid · Electrical vehicle · Fast charging · T-source converter · Battery charging

1 Introduction

Nowadays, EVs are continuously increasing at higher rate for daily transportation purposes. According to the estimates and predictions, more than 125 million EVs will be on road by the year 2030 [1]. Lithium-ion (Li-ion) battery is the core of these innovative vehicles where it stores the energy [2]. Numerous aspects have worked to increase the penetration of renewable sources with EV charging. These aspects are greenhouse gases consequences on environment, continuously reducing PV module prices, rapid technical advancement in EVs [3]. Fuel cell (FC) and solar PV are the outmost capable renewable energy power producing mechanisms. FC has sluggish response and reaction that shall be compensated with super-capacitor bank or battery storage system [4]. Out of various renewable energy sources, FC has been attracting power source for engineers because of its cleanliness, high efficiency and

D. K. Dhaked (✉) · M. Singh · D. Birla
Department of Electrical Engineering, RTU, Kota, India

profitable power source to consumers. The output of FC is DC in nature which can also be directly connected to the solar PV output, and it shall work as backup when standalone microgrid loads are considered [5, 6].

A microgrid system can be defined as an autonomous energy grid which shall operate independently or in parallel with conventional grid. Nowadays, the use of renewable energy resources (RER) integrated with microgrid is used across the world. In microgrid system, BESS is used as key component for stabilizing the voltage fluctuation. Mainly Li-ion battery is used as storage system, but the lifetime of the Li-ion battery is small for stable operation. Thus, to achieve long lifetime operation, a system for charging and discharging a battery is required [7–10]. The major obstruction in moving towards EV is time of recharge, battery size, instability of grid during peak load and inefficient power conversion. The above obstruction can be overcome by use of a system which has less dependency on the grid such as hybrid charging station. Therefore, more research is in practice by researcher and design engineer in the field of RERs connected EV charging system (EVCS) with a battery backup [11, 12]. The modelling of the battery can be classified into three major types. The first type is electrochemical modelling, and it gives high accuracy, but it is difficult to apply. The second type is mathematical modelling, and it can be applied in limited condition. The third and most common type is electrical modelling, and it is mainly used for implementing a battery in a charging system [13, 14].

There are two types of architecture used for charging stations, the first is AC architecture in which AC bus is used, and second is DC architecture in which DC bus is used [15, 16]. The general structure of DC bus architecture is represented in Fig. 1. In this architecture, energy sources are connected at one side of DC bus with the help of DC-DC converter, and another side of loads/charging EV is connected along with DC-DC converter. The converter used in the architecture is bidirectional DC-DC converters. Since last years, academicians and researchers have worked for EV charging methods, architectures and optimizations. Solar PV-based charging method is used for charging stations in [17–19]. Vehicle to grid method was proposed in [20] to sell energy back to grid, and same type of arrangement is described in [21] to inject excess energy to the grid. Paper [22] claims fast functioning outcomes and appropriate application at lower temperature, and reported FC is suitable for backup power with PV source. The architecture of fuel cell can be understood from paper [20]. The operation, control and performance of PV-FC hybrid system are demonstrated in [23]. A comparative study of AC and DC microgrid concept was reported in [24]. It is concluded that DC is more beneficiary because of safe operation, less power electronics (PE) conversion stages, no issues of reactive power control and high energy efficiency. PV-based energy management algorithm-based system is developed in [24]. The design of AC microgrid system also has some issues in synchronization along with frequency handling.

Various converters have already been reported in literature for charging purposes in different architectures, i.e. Z-source converter, multilevel converters [25], single stage bidirectional DC-DC Z-source inverter [26], quasi Z-source bidirectional DC-DC converter [27] and grid tied neutral point clamped [25]. A paper has also reported T-source inverter for solar PV grid tied system [28] that can boost and buck the

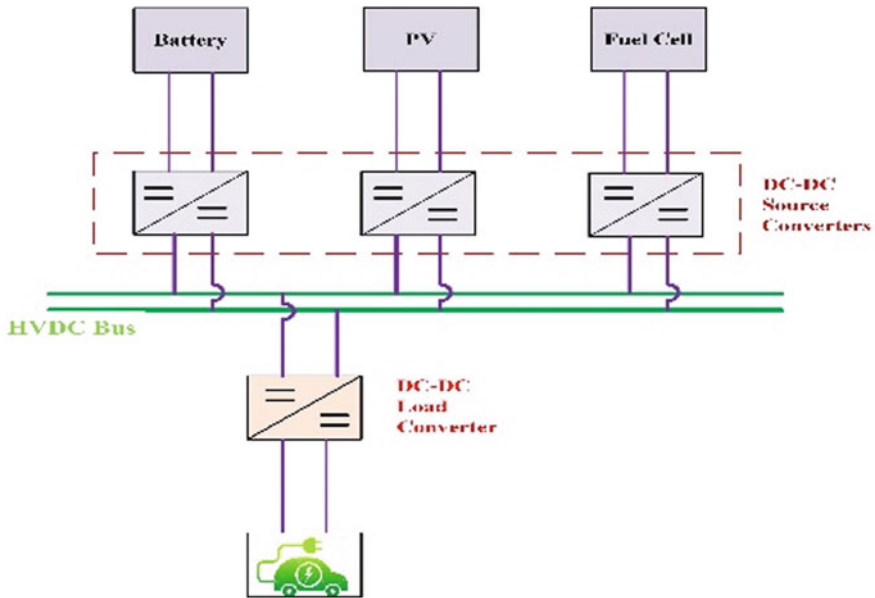


Fig. 1 Microgrid architecture for charging station

voltage according to required level with low output voltage ripple and input voltage along with easy control. A parallel three-level DC-DC converter with an integrated inductor was introduced for EV charging in [29, 30], but it has higher ripples due to high number of switching components, and three-phase hybrid boost converter was employed in [31] for same application that had less switching losses.

Above-mentioned converter had the drawbacks of slow dynamic response, reduced voltage gain because of discontinuous mode of operation, high number of elements that reducing reliability and increasing the switching losses, unable for bidirectional power flow, etc. Hence, the T-source inverter was employed that has less number of switches and conversion stages, fast dynamic response and high gain that motivated authors to work on this topology for EV charging. Various controlling schemes has also employed for control of converters in literature which are as; phase locked loop (PLL) based soft switching technique [32], phase disposition pulse width modulation (PD-PWM) [33], sliding mode control [34], SVPWM PI controller [35, 36] and a cascade two PI controller were used in residential buildings EV charging station [37] that had sluggish dynamic response and resulted in slow charging. Hereafter, getting these above-mentioned controllers, it was concluded that PI controller can filter noise and gives zero steady state error that mainly used in bidirectional control. This paper has also employed modified double PI controller for bidirectional T-source converter (TSC). TSC provides galvanic isolation for converter and loads that enhances voltage stability and power quality, and closed loop control gives lesser current ripples and current THD and gives high voltage gain with double PI controller.

2 Microgrid Arrangement

Fig. 1 shows that battery, solar PV and FC are used as source and TSC is used as DC/DC converter for getting the desired DC voltage level of grid. It has also used T-source bidirectional converter for charging and discharging purposes of EV and buffer battery (Fig. 2).

2.1 T-Source Converter

The TSC is a bidirectional DC-DC converter. The circuit of TSC is designed by combination of *T*-network, LC filter and switch. The *T*-network is formed by connecting two inductors (L_1 and L_2) which are mutually coupled and a capacitor in *T*-shape [38]. This converter is able to provide chosen DC voltage without any dependency on source voltage changes as in solar PV output changes due to weather conditions. The circuit diagram of the TSC is shown in Fig. 3. Depending on the switching condition, TSC is operated in two modes. The first mode of operation is

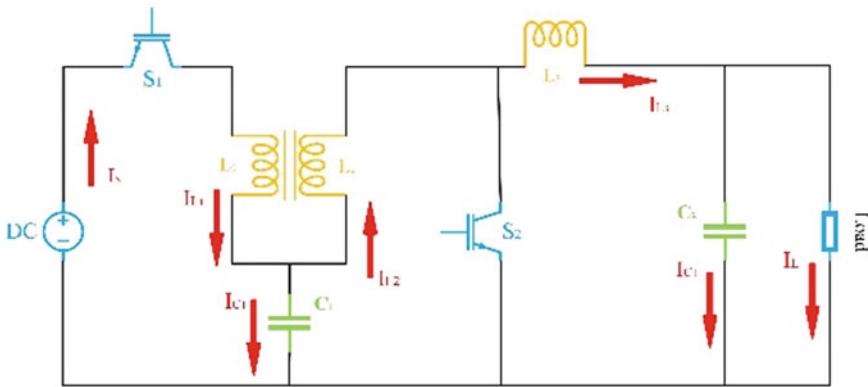


Fig. 2 T-source DC-DC converter circuit diagram

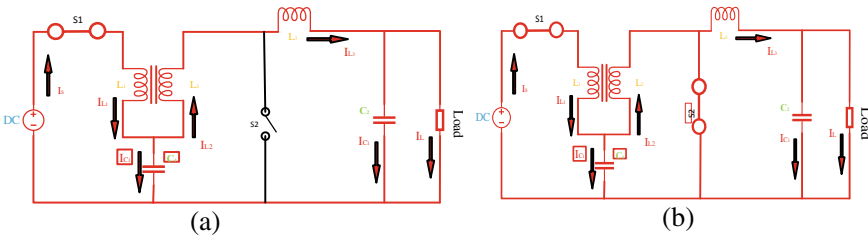
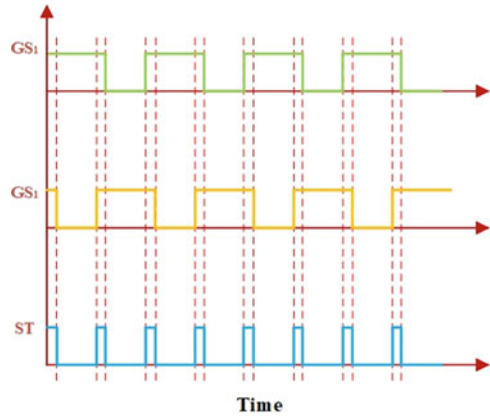


Fig. 3 TSC working modes. a NST mode, b ST mode

Fig. 4 Switching scheme for TSC



non shoot through (NST), while second is shoot through (ST), and the circuit diagram during these modes is shown in Fig. 4a, b, respectively.

During NST mode of operation, the switch S_1 is on, while switch S_2 is off. In this duration, energy is transferred from source side to load side, and output voltage varies according to switch (S_1) duty ratio. Further, inductor of output side is energized, and input current charges the input capacitor. In ST mode, switch S_1 and switch S_2 both are in on state. During this duration, charge stored in capacitor C_1 and capacitor C_2 is transferred to inductor L_2 and inductor L_3 , respectively.

The switching scheme for TSC is shown in Fig. 5, which is obtained from double PI control scheme. In double PI control scheme, both current and voltage are controlled, and hence, it contains very less ripples in output. Here, GS1 is gate pulse for the switch S_1 , GS2 is gate pulse for the switch S_2 , and ST is the shoot-through pulse signal. The duration for which the shoot-through pulse is low is the NST duration, and duration for which it is high is ST duration. The ST duration is the duration for which both the pulse signal GS1 and GS2 are high.

The voltage across capacitors and inductors (assuming both inductor identical) is given in Eqs. (1) and (2), respectively. The voltage across capacitor and inductors is given as

$$V_C = V_{C1} = V_{C2} \tag{1}$$

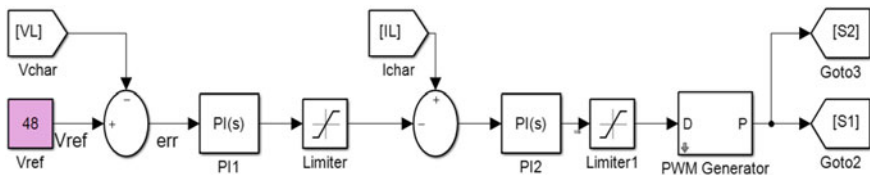


Fig. 5 Double PI control algorithm for T-source DC/DC converter

$$V_L = V_{L1} = V_{L2} \tag{2}$$

During NST mode,

$$V_{L1} = V_S - V_{C1} \tag{3}$$

$$V_d = V_{C1} - V_{L2} = 2V_{C1} - V_S \tag{4}$$

During ST mode, inductor voltage (V_L) and $S2$ voltage (V_d) are as

$$V_d = 0 \tag{5}$$

$$V_{L2} = V_{C1} \tag{6}$$

The switching time over a period is summation of the switching time of NST and ST time and given as shown in Eq. (7).

$$T = T_{nst} + T_{st} \tag{7}$$

By equating inductor voltage to zero over one cycle of period, the capacitor voltage is calculated and given by Eq. (8).

$$V_{C1} = \left(\frac{T_{nst}}{T_{nst} - T_{st}} \right) V_S = \left(\frac{1 - D}{1 - 2D} \right) V_S \tag{8}$$

$$V_{om} = \frac{1}{T} \int_0^T V_d(t) dt = \frac{T_{st} \cdot 0 + T_{nst} (2V_{CZ} - V_S)}{T} \tag{9}$$

The relation between duty ratio and output voltage is given by Eq. (10)

$$V_{oD} = \left(\frac{T_{nst}}{T_{nst} - T_{st}} \right) V_S = \left(\frac{1 - nD}{1 - D(n + 1)} \right) V_S \tag{10}$$

where $D = T_s/T$ is the shoot-through duty cycle ratio of converter.

2.2 Solar PV and Fuel Cell

The solar PV array is considered the most essential and prerequisite sustainable resource due to its free and abundant availability in the atmosphere. The solar power in the model mainly depends upon irradiance and ambient temperature. Solar cell

radiation is measured by air mass, incident angle and radiation to measure cell power (S) given in Eq. 11 below:

The cell power is calculated by the help of Eq. (11)

$$S = M(G_b R_b(\tau\alpha)_b) + G_d(\tau\alpha)_d \frac{1 + \cos\beta}{2} + G_{pg}(\tau\alpha)_g \frac{1 + \cos\beta}{2} \quad (11)$$

Temperature and irradiance are two major factors on which solar power depends as given in Eq. (12).

$$T_{\text{mod}} = T_{\text{air}} + K_T G \quad (12)$$

Equation (13) gives the efficiency of cell

$$\eta_{\text{cell}} = \frac{I_{\text{max}} * V_{\text{max}}}{P_{\text{in}}} \quad (13)$$

The power output is given in Eq. (14) which is a function of temperature.

$$P = P(S, T_{\text{mod}}) \quad (14)$$

Equation (15) gives the cell output power in kWh.

$$P = \frac{P_{\text{peak}} * S}{1000} \quad (15)$$

FC is an electromechanical conversion device, in which electrical energy is produced from chemical energy with water and heat as by-products using H₂ energy. In existing research, proton exchange membrane fuel cell (PEMFC) is used due to its low-temperature operation suitability and quick response. The output voltage and power of fuel cell are calculated by the help of the Eqs. (16) and (17), respectively.

$$V_{\text{FC}} = E - V_{\text{act}} - V_{\Omega} - V_{\text{con}} \quad (16)$$

$$P_{\text{FC}} = N * V_{\text{FC}} * I_{\text{FC}} \quad (17)$$

The efficiency of fuel cell is given by Eq. (18)

$$\eta_{\text{FC}} = \frac{P_{\text{FC}}}{M_{\text{H}_2} \text{HHV}_{\text{H}_2}} \quad (18)$$

Here, M_{H₂} is flow rate of fuel, and P_{FC}, I_{FC} and V_{FC} are FC power output and voltage. Nearly, a FC can yield 0.6–0.75 V, and the power and voltage level can fluctuate from 2 kW to 50 MW and a couple of volts to 10 kV [21], individually relying upon the connections and picked arrangements plan.

3 Simulation Model

The DC microgrid model was designed on MATLAB Simulink tool which has used solar PV, battery and FC as source along with TSC for connecting them to DC link of microgrid. The load or EV for charging was also connected to the DC link with bidirectional TSC. The double PI control scheme was designed for making it closed loop control with voltage and current of battery being charged. The outer voltage control loop regulates the voltage, and the inner loop ensures a ripple free charging current as shown in Fig. 6. Specification for TSC converter is given in Table 1. The battery was charged with each power source at different time, and once all the sources were used for charging the battery. The DC link voltage for microgrid was 48 V, and it is easy to connect each source with DC/DC converter with DC link. Battery used has the energy capacity of 100Ah with 48 V.

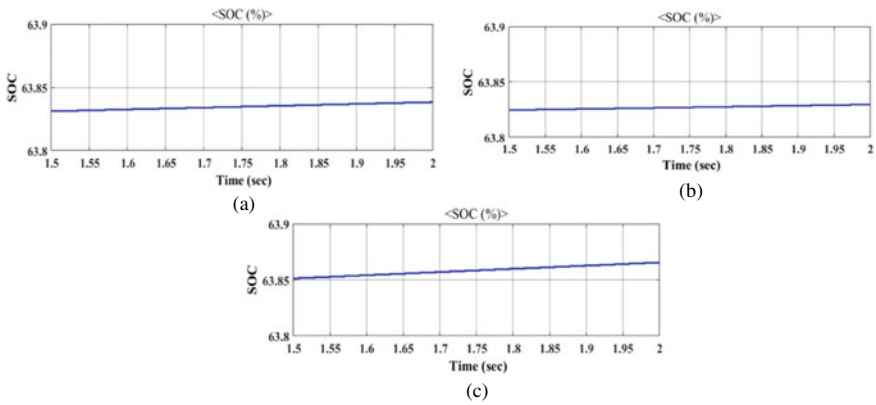


Fig. 6 SOC variation of battery during charge (a) with SPV (b) with FC (c) with DC source

Table 1 Specifications of TSC converter

TSC component	Specification
Switching frequency	2 kHz
Input voltage	200 V
Coupled inductor ratio	1:n
Inductor L_1 and L_2	5 mH
Capacitor C_1	300 μ F
Capacitor C_o	220 μ F

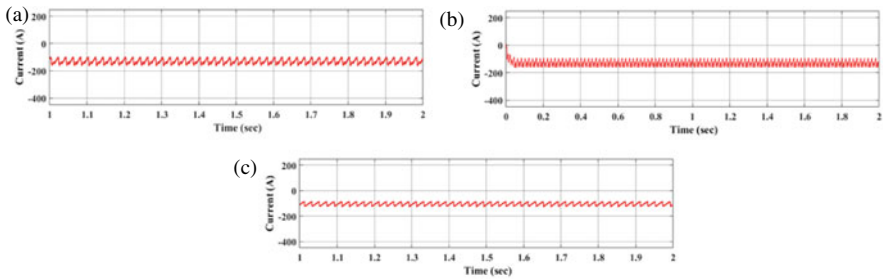


Fig. 7 Current of battery during charge (a) with SPV (b) with FC (c) with DC source

4 Result Analysis

The suggested architecture is designed according to Table 1 with different source of energy. Different sources connected to the battery along with TSC converter are discussed here, and charging performance is analysed in this section. The results obtained for state of charge (SOC) of the battery are represented in Fig. 7 in which Fig. 7a shows the result of battery with SPV source as an input, Fig. 7b shows the result of battery with FC as an input source and Fig. 7c shows the result of battery with DC source as an input. It is observed that battery is charged 0.007% (63.831–63.838%) in duration of 0.5 s (1.5–2.0) when connected with SPV source and is charged 0.005% (63.824–63.829%) in duration of 0.5 s (1.5–2.0) when connected with FC as an input source and charged 0.014% (63.851–63.856%) in duration of 0.5 s (1.5–2.0).

The result obtained for current flowing through battery is represented in Fig. 7 in which Fig. 7a shows the result when SPV is connected as input source and the current flowing is 106.9 A, Fig. 7b shows the result when FC is connected as input source and current flowing is 107.5 A, and Fig. 7c shows the result when DC source is connected as input source and current flowing is 106.7 A.

The result obtained for voltage of battery is represented in Fig. 8 in which Fig. 8a shows the result when SPV is connected as input source and the voltage is 52.47 V, Fig. 8b shows the result when FC is connected as input source and the voltage is 52.28 V, and Fig. 8c shows the result when DC source is connected as an input source and the voltage is 53.19 V.

5 Dynamic Response

The nature of renewable sources and load of the charging structure is variable as the charging vehicles at charging station possess connected/disconnected every time. Hence, it is important to find out the dynamic load checking of this converter. The TSC charging current is around 7–8% higher than conventional buck converter, when

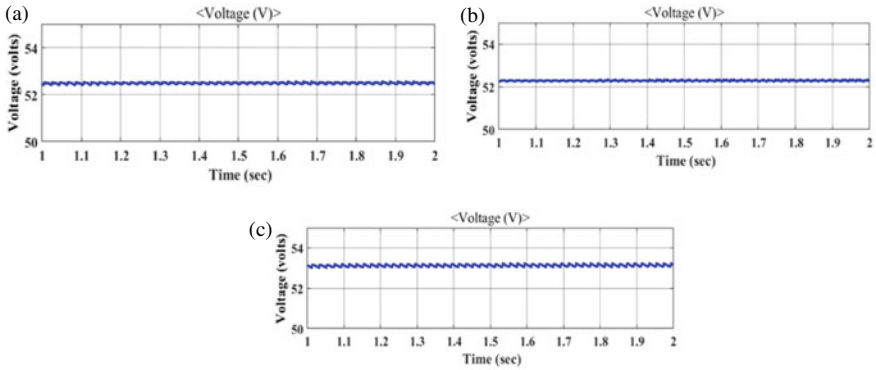


Fig. 8 Voltage of battery during charge (a) with SPV (b) with FC (c) with DC source

checked by comparing as shown in Fig. 9b. Higher gain offered due to impedance network of TSC is the reason behind higher charging current. The charging time reduces with TSC converter integrated charging arrangement as compared to other topologies as given in Table 2.

Figure 9a depicts the TSC charging voltage which is marginally greater than conventional buck converter with less ripples. Switching stress on TSC converter will reduce comparatively by this approach. Charging voltage and current are shown in Fig. 9a, b, and step change response in irradiance from 800 to 600 w/m² for buck and TSC is shown in Fig. 9c. The response time for TSC converter is around 50 ms, while buck converter has 250 ms which is five times higher. Figure 9c shows that at

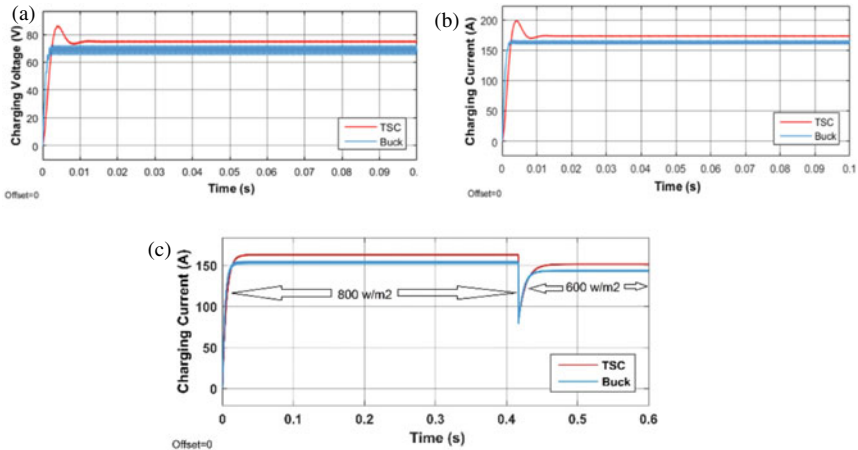


Fig. 9 Dynamic response of TSC. a Charging voltage. b Charging current. c Step change in solar irradiance

Table 2 TSC converter comparison with other DC-DC converter topologies

Parameter	Conventional buck converter	Interleaved boost converter	Z-source DC-DC converter	T-Source DC-DC converter
Gain	Very low	Maximum	High	Very high
Input current THD (%)	8.3	7.2	5.8	3.4
Current ripple (%)	12.5	12.5	<2.5	<2.5
Rise time (%)	1.02	1.08	2.02	1.05
Overshoot	High	Very high	Low	Very low
Charging time	Charging time is high due to low gain property	Charging time is very high	medium	Charging time is low due to high current gain

0.42 s during step change of solar irradiance the response goes for smooth transition for both converters, but it is comparatively less in response of TSC.

6 Conclusion

Fast charging stations are the need of hour for increasing EV on the roads, and TSC converter has been found that it is an ideal converter with double PI controller for charging the EV. This converter provides constant current and voltage for battery charging with low THD, reduced number of switches, less ripple, high gain and fast charging. The designed DC microgrid is also helpful for the charging purposes where the grid availability is not available/possible. DC microgrid with RERs is designed and simulated for EV charging purpose at MATLAB Simulink platform. The charging SOC results with different source of supplies show that the results are satisfactory. The dynamic response is also presented in the study for better understanding, and the fast charging is claimed on the basis of higher charging current, so it will take less time to charge battery than conventional buck converter.

References

1. Di Christopher T (2018) Electric vehicles will grow from 3 million to 125 million by 2030. International Energy Agency forecasts, CNBC
2. Dhaked DK, Gopal Y, Birla D (2019) Battery charging optimization of solar energy based telecom sites in India. Eng Technol Appl Sci Res 9(6):5041-5046
3. Bhagiya RD, Patel RM (2019) PWM based double loop PI control of a bidirectional DC-DC converter in a standalone PV/battery DC power system. In: 2019 IEEE 16th India Council International Conference (INDICON), pp 1–4, Dec 2019

4. Hosseini M, Dincer I, Rosen MA (2013) Hybrid solar–fuel cell combined heat and power systems for residential applications: energy and exergy analyses. *J Power Sour* 221:372–380
5. Kirubakaran A, Jain S, Nema RK (2009) A review on fuel cell technologies and power electronic interface. *Renew Sustain Energy Rev* 13(9):2430–2440
6. Samy MM, Barakat S, Ramadan HS (2019) A flower pollination optimization algorithm for an off-grid PV-fuel cell hybrid renewable system. *Int J Hydrogen Energy* 44(4):2141–2152
7. Deblecker O, Stevanoni C, Vallee F (2016) Cooperative control of multi-functional inverters for renewable energy integration and power quality compensation in micro-grids. In: 2016 International symposium on power electronics, electrical drives, automation and motion (SPEDAM). IEEE, June 2016, pp 1051–1058
8. Dong J, Gao F, Guan X, Zhai Q, Wu J (2016) Storage-reserve sizing with qualified reliability for connected high renewable penetration micro-grid. *IEEE Trans Sustain Energy* 7(2):732–743
9. Fernandes NT, Demonti R, de Andrade J, de Melo PF, Bianchin CG, de Almeida AR, Lemos AR (2015) Control strategy for pulsed lead acid battery charger for stand-alone photovoltaics. In: 2015 IEEE 13th Brazilian power electronics conference and 1st southern power electronics conference (COBEP/SPEC). IEEE, pp 1–6, Nov 2015
10. Singh RK, Mishra S (2012) A digital optimal battery charger with the inbuilt fault detection property. In: 2012 IEEE international conference on power electronics, drives and energy systems (PEDES). IEEE, pp 1–6, Dec 2012
11. Gjelaj M, Hashemi S, Traeholt C, Andersen PB (2018) Grid integration of DC fast-charging stations for EVs by using modular li-ion batteries. *IET Gener Transmiss Distr* 12(20):4368–4376
12. Khan W, Ahmad F, Alam MS (2019) Fast EV charging station integration with grid ensuring optimal and quality power exchange. *Eng Sci Technol Int J* 22(1):143–152
13. Li X, Xiao M, Malinowski K, Choe S-Y (2011) State-of-charge (SOC) estimation based on reduced order of electrochemical model for a pouch type high power Li-polymer battery. In: Proceedings of the 7th IEEE vehicle power and propulsion conference (VPPC '11), pp 1–6, Chicago, Ill, USA, Sept 2011
14. Li S, Ke B (2011) Study of battery modeling using mathematical and circuit oriented approaches. In: 2011 IEEE Power and Energy Society General Meeting. IEEE, July, pp 1–8
15. Bai S, Lukic SM (2013) Unified active filter and energy storage system for an MW electric vehicle charging station. *IEEE Trans Power Electron* 28(12):5793–5803
16. Rivera S, Wu B, Wang J, Athab H, Kouro S (2013) Electric vehicle charging station using a neutral point clamped converter with bipolar DC bus and voltage balancing circuit. In: IECON 2013-39th annual conference of the IEEE Industrial Electronics Society. IEEE, Nov 2013, pp 6219–6226
17. Le T, Phung BN (2021) Load shedding in microgrids with consideration of voltage quality improvement. *Eng Technol Appl Sci Res* 11(1):6680–6686
18. Guo Y, Xiong J, Xu S, Su W (2015) Two-stage economic operation of microgrid-like electric vehicle parking deck. *IEEE Trans Smart Grid* 7(3):1703–1712
19. Mouli GC, Bauer P, Zeman M (2016) System design for a solar powered electric vehicle charging station for workplaces. *Appl Energy* 168:434–443
20. Van Roy J, Leemput N, Geth F, Büscher J, Salenbien R, Driesen J (2014) Electric vehicle charging in an office building microgrid with distributed energy resources. *IEEE Trans Sustain Energy* 5(4):1389–1396
21. Alam M, Kumar K, Verma S, Dutta V (2020) Renewable sources based DC microgrid using hydrogen energy storage: modelling and experimental analysis. *Sustain Energy Technol Asses* 42:100840
22. Ghosh PC, Emonts B, Janßen H, Mergel J, Stolten D (2003) Ten years of operational experience with a hydrogen-based renewable energy supply system. *Sol Energy* 75(6):469–478
23. Lotfi H, Khodaei A (2015) AC versus DC microgrid planning. *IEEE Trans Smart Grid* 8(1):296–304
24. Mohamed A, Salehi V, Ma T, Mohammed O (2013) Real-time energy management algorithm for plug-in hybrid electric vehicle charging parks involving sustainable energy. *IEEE Trans Sustain Energy* 5(2):577–586

25. Rivera S, Wu B, Kouro S, Yaramasu V, Wang J (2014) Electric vehicle charging station using a neutral point clamped converter with bipolar DC bus. *IEEE Trans Ind Electron* 62(4):1999–2009
26. Omran KC, Mosallanejad A (2018) SMES/battery hybrid energy storage system based on bidirectional Z-source inverter for electric vehicles. *IET Electr Syst Transp* 8(4):215–220
27. Zhang Y, Liu Q, Gao Y, Li J, Sumner M (2018) Hybrid switched-capacitor/switched-quasi-Z-source bidirectional DC–DC converter with a wide voltage gain range for hybrid energy sources EVs. *IEEE Trans Ind Electron* 66(4):2680–2690
28. Sivaraman P, Prem P (2017) PR controller design and stability analysis of single stage T-source inverter based solar PV system. *J Chin Inst Eng* 40(3):235–245
29. Tan L, Zhu N, Wu B (2015) An integrated inductor for eliminating circulating current of parallel three-level DC–DC converter-based EV fast charger. *IEEE Trans Ind Electron* 63(3):1362–1371
30. Prabhakar S, Febin Daya JL (2016) A comparative study on the performance of interleaved converters for EV battery charging. In: 2016 IEEE 6th International conference on power systems (ICPS). IEEE, pp 1–6, Mar 2016
31. Tazay A, Miao Z (2018) Control of a three-phase hybrid converter for a PV charging station. *IEEE Trans Energy Convers* 33(3):1002–1014
32. Reis FE, Bascopé RP, Tofoli FL (2018) Bidirectional three-phase 3L-SNPC converter for EV charging stations. In: 2018 13th IEEE International conference on industry applications (INDUSCON). IEEE, pp 298–304, Nov 2018
33. Ibanez FM, Echeverria JM, Astigarraga D, Fontan L (2015) Soft-switching forward DC–DC converter using a continuous current mode for electric vehicle applications. *IET Power Electron* 8(10):1978–1986
34. Serna-Garcés SI, González Montoya D, Ramos-Paja CA (2018) Control of a charger/discharger DC/DC converter with improved disturbance rejection for bus regulation. *Energies* 11(3):594
35. Lai CM, Cheng YH, Hsieh MH, Lin YC (2017) Development of a bidirectional DC/DC converter with dual-battery energy storage for hybrid electric vehicle system. *IEEE Trans Veh Technol* 67(2):1036–1052
36. Qu KQ, Niu QQ, Yang C, Zhao JB (2013) Battery charge-discharge control strategy based on the single Z-source three-level SVPWM inverter. In: 2013 IEEE International conference on applied superconductivity and electromagnetic devices. IEEE, pp 30–33
37. De Melo HN, Trovao JPF, Pereirinha PG, Jorge HM, Antunes CH (2017) A controllable bidirectional battery charger for electric vehicles with vehicle-to-grid capability. *IEEE Trans Veh Technol* 67(1):114–123
38. Prem P, Sivaraman P, Sakthi Suriya Raj JS, Jagabar Sathik M, Almakhlles D (2020) Fast charging converter and control algorithm for solar PV battery and electrical grid integrated electric vehicle charging station. *Automatika* 61(4):614–625